ELSEVIER

Physica D 116 (1998) 244–252

PHYSICA D

Laplacian growth as one-dimensional turbulence

M.B. Hastings, L.S. Levitov *

Physics Department, 12-134d, 77 Massachusetts Ave., Massachusetts Institute of Technology, Cambridge, MA 02139, USA

Received 6 December 1996; received in revised form 19 May 1997; accepted 30 September 1997
Communicated by C.K.R.T. Jones

Abstract

A new model of Laplacian stochastic growth is formulated using conformal mappings. The model describes two growth regimes, stable and turbulent, separated by a sharp phase transition. The first few Fourier components of the mapping define the web, an envelope of the cluster. The web is used to study the transition and the dynamics of large-scale features of the cluster characterized by evolution from macro- to micro-scales. Also, we derive scaling laws for the cluster size. Copyright © 1998 Elsevier Science B.V.

PACS: 64.60.Ak; 05.20.Dd; 41.10.Dq
Keywords: Stochastic growth; Diffusion limited aggregation

The relation of the two kinds of Laplacian dynamics, stochastic [5] and deterministic [15], represents a very interesting problem. In the stochastic dynamics, such as diffusion-limited growth [18], dielectric breakdown [13], or fracturing, the cluster grows by particles diffusing and sticking to it, or by emanating lightning strikes, or cracks, with probabilities determined from Laplace's equation. The growing cluster is a scale-invariant fractal object with non-trivial geometric characteristics that have been extensively explored by a combination of numerical and analytical methods [4,7,13,14]. In deterministic growth [15], exemplified by the Hele-Shaw dynamics, the boundary of the growing object moves with a local velocity determined by Laplace's equation. In this problem, attention was focused on the fingering instability, which at small capillary effects leads to fractal-like patterns [2,17] resembling DLA cluster. To draw an explicit relation of the two large-scale structures, however, turns out to be difficult, even numerically.

A natural way to proceed would be to study the continuum limit of stochastic growth, which appears to be non-trivial. Taking DLA as an example [14], the arising difficulty is that the naive continuum limit, understood as taking the particle size to be zero, gives Hele–Shaw dynamics with zero surface tension [16], leading to finite-time singularities. In that, Laplacian growth has a lot of similarity with turbulence. The finite-time singularities conjectured for Euler dynamics of an ideal fluid are essential for understanding turbulent flow [3]. The large-scale spectrum of velocity fluctuations in the flow is determined by the instability cascade in inertial range, with viscosity and thermal noise being relevant only on microscale, where the singularities are resolved. Also, in parallel with energy conservation in the inertial range of Euler dynamics, it

* Corresponding author. E-mail: Levitov@mit.edu.

PII S0167-2789(97)00244-3

is found that all integrals of Hele–Shaw dynamics are conserved in DLA growth as well, up to small fluctuations arising on microscale [12]. From that, it is natural to conjecture that the large-scale DLA dynamics is equivalent to Laplacian contour dynamics, with the finite-time singularities being resolved on microscale due to noise.

In order to explore this similarity, we propose a new class of models, continual rather than lattice-like, that provides an explicit connection between stochastic growth and contour dynamics. The growth is represented as a random sequence of conformal maps with memory, which facilitates numerical and analytical treatment. (It has been shown [4] that conformal maps simplify analysis of the mass distribution in the conventional DLA problem.) In this model there are different parameter regimes analogous to the low and high Reynolds fluid dynamics: weakly stochastic, macroscopically stable growth, and noise-driven turbulent growth. The transition between the two regimes is sharp. By varying the "Reynolds" parameter, one can model several known growth problems such as dielectric breakdown and DLA.

Stating the problem. One step of Laplacian growth involves attaching a new object to the cluster with a probability determined by the solution, outside the cluster, of Laplace's equation $\nabla^2 u = 0$, with boundary conditions

$$\begin{aligned} &u = 0, && \text{at the cluster boundary,} \\ &u = \frac{1}{2\pi}\ln(r), && \text{as the radial coordinate , } r \to \infty. \end{aligned} \tag{1}$$

The probability for the new object to appear within the interval $\mathrm{d}l$ of the boundary is given by

$$\mathrm{d}P = |\nabla u|\,\mathrm{d}l. \tag{2}$$

The size of the new object (quantified by its area) can be

(a) Constant, as in DLA,
(b) Proportional to some power of local field, as in dielectric breakdown. For reasons made clear later we choose to write the power as $\alpha - 2$, so that the area $\sim |\nabla u|^{\alpha-2}$.

Also, there is a freedom to choose different shapes for the object. To model breakdown and fracturing problems, where an individual growth step is a lightning strike, or a crack, we consider growth that involves one-dimensional objects (hereafter called "strikes"). For diffusion-controlled growth, it is more natural to take new objects roughly equal in all dimensions (called "bumps").

In the canonical lattice model of dielectric breakdown [13] the size of a new object is fixed, but the sticking probabilities are given by a power law:

$$\mathrm{d}P = |\nabla u|^{\eta}\,\mathrm{d}l. \tag{3}$$

To relate it with our model, one compares local area growth rates, and finds $\eta = \alpha - 1$. Given that, and assuming that universality classes are determined only by the local area growth law, we expect that the two models lead to the same macroscopic properties. Relation to DLA, known to be a particular case of dielectric breakdown with $\eta = 1$, is thus expected at $\alpha = 2$. However, the relation of the lattice and the mapping models, although confirmed by simulations, needs to be explored further.

The physical significance of α can be seen as similar to that of η in the dielectric breakdown model. They are both phenomenological parameters introduced to represent a larger range of growth processes. However, the strike-models we introduce with $\alpha < 1$ produce a class of patterns not described by the dielectric breakdown model for any η. As seen in Fig. 1, we are able to produce shapes which are microscopically very complicated, but which have a smooth, approximately circular boundary. One may see something similar in some dielectric breakdown and cracking experiments. See, e.g., the discussion in Chapter 10.4 of Vicsek's book [5]. Within our model, the significance of α is that it permits us to vary across a range of growth regimes from stable growth to unstable, turbulent growth.

Mapping representation of growth. We represent the cluster by a conformal mapping $F(z)$ of the exterior of the disk $|z| \geq 1$ to the exterior of the object. (Uniqueness up to reparametrization follows from the Riemann mapping theorem.) To describe the change of the mapping F due to a single new object added to the cluster we use the mapping $f_{\lambda,\theta}(z)$ that maps the domain $|z| \geq 1$ onto a sub-domain by attaching a

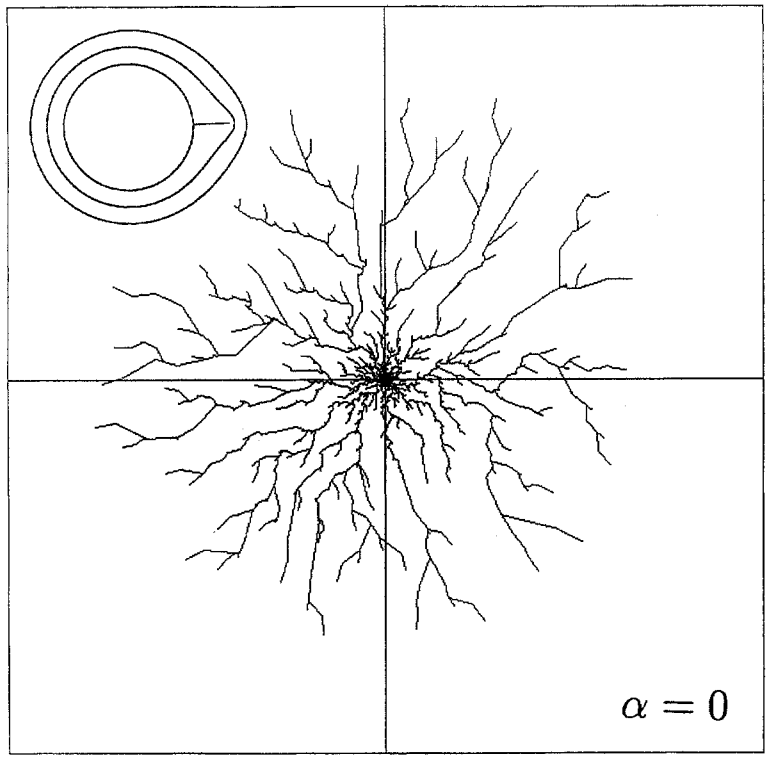

Fig. 1. Cluster grown using strike mappings with $\alpha = 0$. Inset: A strike map applied to three circles of varying radii.

strike or a bump to the boundary at $z = e^{i\theta}$ (see insets of Figs. 1 and 2). The strike-mapping $f_{\lambda,\theta}(z)$ is

$$e^{i\theta} f_\lambda(e^{-i\theta} z), \tag{4}$$

where f_λ is given by

$$\frac{1+\lambda}{2z}(z+1)\left(z+1+\sqrt{z^2+1-2z\frac{1-\lambda}{1+\lambda}}\right)-1, \tag{5}$$

where λ is a parameter describing the size of the strike. Below, we use only mappings with $\lambda \ll 1$, in which case the strike length is $2\sqrt{\lambda} + O(\lambda^{3/2})$. The bump-mapping can be chosen in several ways. We use

$$f_{\text{bump}}(z) = z^{1-a} f^a_{\text{strike}}(z), \tag{6}$$

$0 < a < 1$. The growth is described by composition of mappings

$$F_i(z) = F_{i-1}(f_{\lambda_i,\theta_i}(z)), \tag{7}$$

where the single step mappings $f_{\lambda_i,\theta_i}(z)$ can be (5) or (6). Note that the order of the functions in the composition is reversed with respect to the growth time sequence.

Now we determine the dependence of the parameters θ_i and λ_i on the growth step. From conformal invariance of the two-dimensional Laplacian it follows that the random numbers θ_i are uniformly distributed in the interval $0 \le \theta \le 2\pi$, and uncorrelated. For λ_i, the power law relationship of the new object area, A, and local field,

$$A \sim |\nabla u|^{\alpha-2} \tag{8}$$

gives

$$\lambda_i = \lambda_0 |\, dF_{i-1}/dz|^{-\alpha}_{z=e^{i\theta_i}}. \tag{9}$$

(To obtain (9) one just writes the Laplace's problem solution in terms of the mapping $u(z) = u_0 \operatorname{Re} \ln F(z)$.) Using (9) and the composition rule (7) one can grow

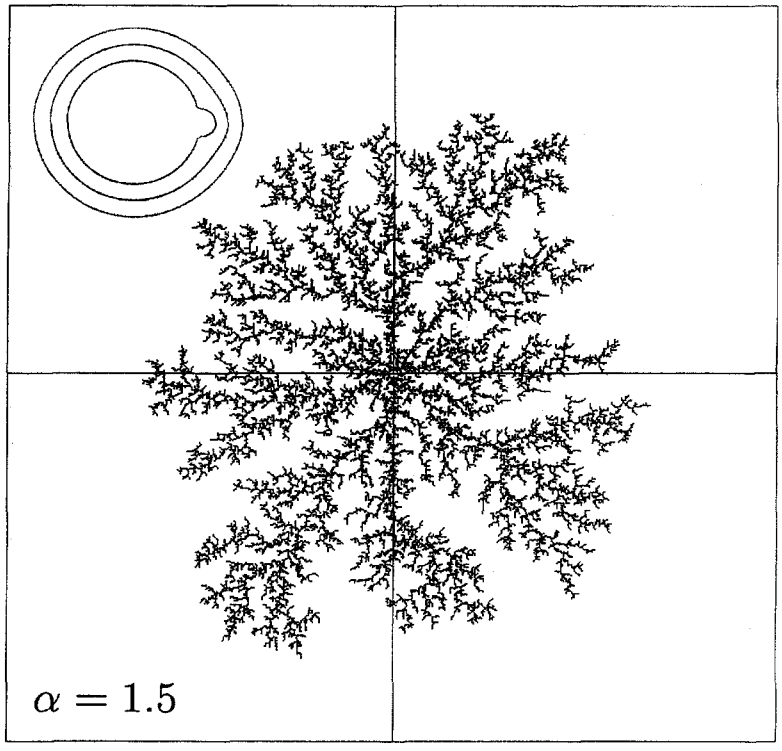

Fig. 2. Cluster grown using bump mappings with $\alpha = 1.5$. Inset: A bump map applied to three circles of varying radii.

the object without solving Laplace's equation at each step.

Using (7) and (9), we simulate the growth. The examples of growth patterns obtained for $\alpha = 0,\ 1.5,\ 2$ are shown in Figs. 1–3. In the simulation, the data that represent the structure are the set of angles θ_i, and the set of λ_i. For N growth steps, the algorithm complexity is N^2, which compares quite favorably to the canonical dielectric breakdown model (e.g., see [1]), and comes close to the best algorithms known for the DLA model.

There is a special parameter value $\alpha = 0$ at which the model (7), (9) is *conformally invariant*, which means that the stochastic dynamics commutes with arbitrary conformal transformations. As a result, at $\alpha = 0$ the growth does not have any "memory": according to Eq. (9), all λ_i are the same, and thus all mappings $f_{\lambda_i,\theta_i}(z)$ are uncorrelated. As α increases from 0 to higher values, the memory effects become stronger and eventually lead to non-trivial dynamics.

The web. To gain some insight, it is useful to consider power series expansions in z^{-1} for $F_n(z)$ and $f_{\lambda_n,\theta_n}(z)$:

$$F_n(z) = a_1^{(n)} z + a_0^{(n)} + a_{-1}^{(n)} z^{-1} + \cdots, \tag{10}$$

$$f_{\lambda_n,\theta_n}(z) \approx (1+\lambda_n)z + \sum_{k=1}^{O(1/\sqrt{\lambda})} 2\lambda_n e^{ik\theta_n} z^{1-k}, \tag{11}$$

asymptotically equal to

$$z + \lambda_n z(z + e^{i\theta_n})/(z - e^{i\theta_n}). \tag{12}$$

In the expansion for f we keep only low order terms in λ_n, since we are going to work with small λ_n. Although to linear order the cutoff in (11) is infinite, the finite cutoff is written in explicitly to indicate that f has some smallest scale, beyond which it is smooth (see below).

By truncating the series (10) one obtains a function that maps the domain $|z| > 1$ to an envelope of the grown cluster (we call it the *web*). The web, even

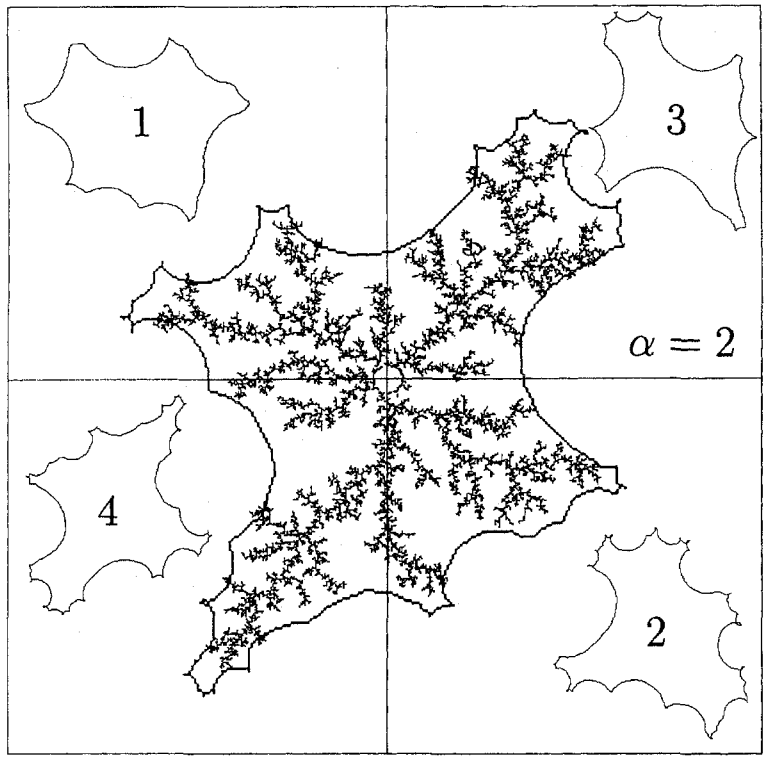

Fig. 3. Cluster grown using bump mappings with $\alpha = 2$, and its web obtained by truncating the cluster mapping series expansion at 40 terms. Insets 1 and 2: Examples of growth using the web dynamics with 20 and 40 terms. Insets 3 and 4: For comparison, the webs of the clusters grown using exact mapping obtained by truncating at 20 and 40 terms.

for a relatively small number of terms, is an accurate representation of the cluster (see Fig. 3). The web is sensitive to the structure of the outer growing part of the cluster, rather than to the stationary inner region, which makes the web a useful tool. One observes a change in the web grown at different α. For $0 \leq \alpha < 1$ the web is rounded, becoming more circular at large times. On the other hand, at $1 < \alpha \leq 2$ the web is rough at all times, the roughness scaling as the cluster size.

An alternative way of imaging the growing cluster used in the literature is based on the averaged occupancy [2]. Its relation to the web represents an interesting problem.

The web dynamics. Next, we define *web dynamics*. To obtain the web for a given cluster requires a numerical Fourier transform. Using expansions (10) and (11) and rules (7) and (9), we can instead directly evolve the power series, calculating new coefficents of the series from old coefficients. To do this, (10) must be cutoff at some fixed number of terms. As long as this cutoff is greater than the cutoff in (11), the web dynamics yields good results. Even for a relatively small number of terms (say, 20–50), it agrees acceptably with the exact dynamics, both in the size of the cluster taken as function of time, and in the overall shape. Several examples of grown webs are shown in the insets of Fig. 3. Details on the web dynamics algorithm will be published elsewhere [9].

One advantage of the web dynamics is that it takes much fewer computer steps than exact dynamics. Also, the web can be used to study the large-scale limit of the growth dynamics. If for any reason one is only interested in macroscopic characteristics, such as the overall growth rate, or the roughness of the cluster boundary, then the web is a more appropriate

instrument than exact mapping. Finally, the web provides a bridge between exact dynamics and its continuum limit (see below).

Taking continuum limit. Consider a continuum limit in which the attached objects are infinitesimally small. Then the growth is described by *deterministic* equation written for $F(z)$. To derive it we can use the power series (11). First, substitute expansion (11) of $f_{\lambda_n,\theta_n}(z)$ in the recursion relation (7), and expand in λ_n: $F_{n+1}(z) = F_n(z) + \delta F_n(z)$, where

$$\delta F_n(z) = \frac{\partial F_n(z)}{\partial z}\lambda_n z\frac{z+e^{i\theta_n}}{z-e^{i\theta_n}}. \tag{13}$$

Then the continuum limit is implemented by averaging over θ_n. Taking the integral over $d\theta_n$ and substituting $\lambda_n = \lambda_0|F_z|^{-\alpha}$, gives Shraiman–Bensimon equation

$$\dot{F}(z) = \lambda_0 z F_z(z)\oint |F_z(e^{i\theta_n})|^{-\alpha}\frac{z+e^{i\theta_n}}{z-e^{i\theta_n}}\frac{d\theta_n}{2\pi} \tag{14}$$

where we write F_z for dF_n/dz. For $\alpha = 2$, which corresponds to constant area of attached object, i.e., to DLA, we recover the Hele–Shaw problem which has rich analytic properties [16] and can be solved in terms of poles of $F(z)$ moving within the disk $|z| < 1$. It turns out that generic dynamics leads to singularities occurring at finite time:

$$F(z,t) \sim A(t)/(z - w(t)), |w(t \to t_0)| \to 1. \tag{15}$$

Let us compare this behavior with the web dynamics. The singularities of dynamics (14) can be recognized in the cusp-like features appearing on the web (see Fig. 3). After appearing, they become sharper, but later, instead of developing into real singularities, they just disappear being gradually replaced by other similar features nearby.

It is easy to draw a parallel with the currently accepted picture of turbulence [3]. In the inertial range, the fluid dynamics gives rise to singular vortex filaments. In the absence of viscosity these would develop into singularities. However, on the viscous range the singularity is suppressed, and thus a turbulent flow exhibits a random sequence of singular-like structures replacing each other.

In the web, the analog of the spatial scale is the power of z. It can thus be said that sharpening of the cusps on a web corresponds to the shift to smaller scale. Cusps are suppressed at microscale set by the largest power of z in (11). This shortest scale is determined by the value of λ, which corresponds to the amount of noise; in the continuum limit the noise vanishes and the microscale becomes infinitely small. In the case of web dynamics, the truncation of (10) may also fix a microscale. In both cases, for the exact mapping and for the web, we have singular-like structures developing in the "inertial range", where the continuum equation (14) holds, evolving to shorter scales, and disappearing there. It is thus appropriate to call the long-time dynamics turbulent.

The role of the noise due to the particle discreteness is unusual. The dynamics without noise would by itself produce chaos, and even singularities. The noise suppresses singularities, and makes the system run forever, similar to the role of viscosity in a turbulent flow. Such behavior can be contrasted to other stochastic growth problems, such as the Kardar–Parisi–Zhang dynamics [10], or kinetic roughening of stable Laplacian fronts [11], where all stochastic properties arise due to the noise. In such problems, naive continuum limit gives rise to stable dynamics, and thus is nonproblematic.

Phase transition. As function of α, there is a transition at $\alpha = 1$ from stable to turbulent growth. The stable growth at $\alpha < 1$ is similar for the strike- and the bump-models: the degree of roughness of the cluster boundary, scaled in the cluster size, decreases with time.

The transition at $\alpha = 1$ is sharp. To verify this, we plot the mean square of the fluctuations of the boundary rescaled by the object size (see Fig. 4). Here, we grew the object on a periodic strip of finite width instead of the circular geometry discussed above, and used the first Fourier component of the mapping as a measure of fluctuations. As the bump size λ_0 becomes smaller, the fluctuations decrease at $\alpha < 1$, indicating convergence to the continuum limit (14), but remain finite at $\alpha > 1$.

These results may not exactly apply to the circular cluster growth, due to certain differences in DLA growth in the two geometries. In contrast with the circular growth, in the long-time limit, the growth in

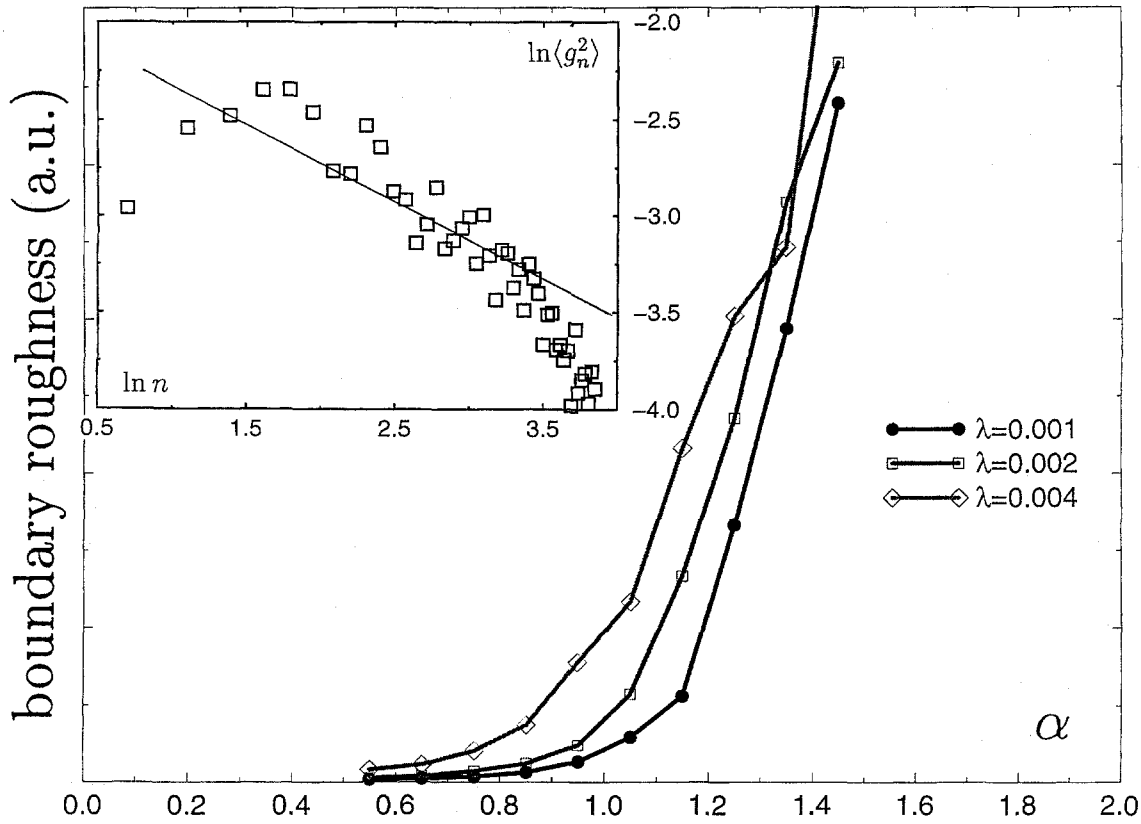

Fig. 4. Boundary roughness measured by the mean square value of the first Fourier coefficient for three different values of λ_0. Inset: Mean squares of Fourier coefficients of F_z^{-1} scaled by the cluster size a_1, averaged over 50 runs. Theoretical line with the slope $-\frac{2}{5}$ is drawn.

the strip geometry is statistically unchanging, which is why this geometry was selected for the phase transition study.

One may easily understand this phase transition by a simple analytical argument. Writing down a power series expansion for F in the strip geometry in analogy with Eq. (10) for the circular geometry, one obtains

$$F_n(z) = z + a^{(n)} + a_{-1}^{(n)} e^{iz} + a_{-2}^{(n)} e^{2iz} + \cdots, \qquad (16)$$

where the mapping is defined for $\mathrm{Im}(z) > 0$ and the mapping is periodic when z is replaced by $z + 2\pi$. If one then converts the continuum equation of motion (14) to the strip geometry, and linearizes the resulting nonlinear equation about small values of a_{-k}, one obtains the result that for $k > 0$

$$\dot{a}_{-k} = k(\alpha - 1)a_{-k}. \qquad (17)$$

Then, for $\alpha < 1$, the linear equation of motion is stable, while for $\alpha > 1$, the linear equation of motion is unstable.

The turbulent growth at $\alpha > 1$ is sensitive to the model. In the strike-models the object grows by emanating long chains of strikes (macro-strikes), which contain almost all the density at $\alpha > 1$.

For the bump-models, at $\alpha > 1$ the growing object forms a self-similar fractal cluster, with the fractal dimension varying with α (see Figs. 2 and 3). The self-similarity was checked by calculating gyration radius, which is found to be a power law function of time, and by calculating fractal dimension using the box counting method. The box counting fractal dimension was slightly lower, but was consistent with the gyration radius power law. The difference is most likely due to the small sampe size (approximately 10 000 steps).

The cluster grown at $\alpha = 2$ has properties identical to that of a DLA cluster. This is expected, since at $\alpha = 2$ the new object size remains roughly constant throughout the growth. So, the $\alpha = 2$ bump models are equivalent to DLA.

Scaling laws. Given the self-similarity of DLA, it is of interest to study scaling of the power series coefficients. For that we use the expansion of

$$F_z^{-1} = g_0 + g_1 z^{-1} + \cdots \tag{18}$$

This function, F_z^{-1}, is the analytic function whose absolute value gives the local electric field. The mean square of g_n's is plotted against n on a log–log plot (see inset to Fig. 4). This plot is specific to $\alpha = 2$. A renormalization group theory developed elsewhere [8] predicts the slope of $-\frac{2}{5}$, also shown in the plot. The higher Fourier coefficients have a large effect on the growth rate of the cluster, as discussed below.

Using (7), the first term of the series for F_n can be written in closed form:

$$a_1^{(n)} = \prod_{0<j\leq n} (1 + \lambda_j). \tag{19}$$

The geometric meaning of $a_1^{(n)}$ is the size of the cluster.

For $\alpha < 1$, the object is roughly circular, and λ_j is determined by a_1. Noise in the higher components leads to some renormalization of $\lambda_0 \to \tilde{\lambda}_0$, and then

$$\lambda_j = \tilde{\lambda}_0 (a_1^{(j-1)})^{-\alpha}. \tag{20}$$

This equation has a power law solution:

$$a_1^{(n)} = (1 + \alpha \tilde{\lambda}_0 n)^{1/\alpha}. \tag{21}$$

The same power law exponent can be found from the circular-symmetric solution to Eq. (14).

In our simulation, at any α the growth of a_1 is indeed described by a power law, and at $\alpha < 1$, the power law exponent is equal to $1/\alpha$, as predicted by Eq. (21). However, at $\alpha \geq 1$, the exponent is somewhat larger than $1/\alpha$, and the deviation increases at larger α. This correction is due to the growth of the higher Fourier components. Any given one of the higher Fourier components eventually stabilizes at some average value, but as the object grows, higher and higher Fourier components contribute to λ, and the renormalization of λ_0 in Eq. (21) increases with time, leading to a correction in the exponent.

Even at large α it is still true that, on an average,

$$da_1/dt = \lambda a_1 \tag{22}$$

and so, since a_1 follows a power law in time, the average of λ scales as t^{-1}. This is equivalent to the electrostatic scaling law derived by Halsey [6]

In summary, we studied analytic models of Laplacian stochastic growth, formulated in terms of conformal mappings, and characterized by two growth regimes: stable ($\alpha < 1$) and turbulent ($\alpha > 1$), the transition at $\alpha = 1$ being sharp. By truncating the series expansion of the mapping, we defined the web, geometric envelope of growing cluster. The web dynamics is used to demonstrate a relation between transient features of the turbulent growth and finite-time singularities of the deterministic problem. The turbulent growth bump-models are found to be equivalent to the dielectric breakdown and DLA models.

This work was initiated by discussions with Boris Shraiman.

References

[1] C. Amitrano, Phys. Rev. A 39 (1989) 6618.
[2] A. Arneodo et al., Phys. Rev. Lett 63 (1989) 984.
[3] S. Douady, Y. Couder, M.E. Brachet, Phys. Rev. Lett. 67 (1991) 983; A. Pumir, E.D. Siggia, Phys. Fluids 30 (1987) 1606; Phys. Fluids A2 (1990) 220; A.J. Chorin, Comm. Mat. Phys. 83 (1982) p. 517;
[4] J.P. Eckmann et al., Phys. Rev. Lett. 65 (1990) 52; Phys. Rev. A 39 (1989) 3185.
[5] A. Erzan, L. Pietronero, A. Vespignani, Rev. Mod. Phys. 67 (1995) 545; T. Vicsek, Fractal Growth Phenomena, World Scientific, Singapore, 1992; H.E. Stanley, N. Ostrowsky, (Eds.), On Growth and Form, Nijhoff, Dordrecht, 1986.
[6] T.C. Halsey, Phys. Rev. Lett. 59 (1987) 2067.
[7] T.C. Halsey, M. Leibig, Phys. Rev. A 46 (1992) 7793; T.C. Halsey, Phys. Rev. Lett. 72 (1994) 1228.
[8] M.B. Hastings, Renormalization theory of stochastic growth, Phys. Rev. E 55 (1997) 135.
[9] M.B. Hastings, L.S. Levitov, to be published.
[10] M. Kardar, G. Parisi, Y.C. Zhang, Phys. Rev. Lett. 56 (1986) 889.
[11] J. Krug, P. Meakin, Phys. Rev. Lett. 66 (1991) 703.
[12] M.B. Minneev-Weinstein, R. Mainieri, Phys. Rev. Lett. 72 (1994) 8803.

[13] L. Niemeyer, L. Pietronero, H.J. Wiessmann, Phys. Rev. Lett. 52 (1984) 1033; L. Pietronero, H.J. Wiessmann, J. Stat. Phys. 36 (1984) 909.
[14] G. Parisi, Y.C. Zhang, J. Stat. Phys. 41 (1985) 1; L. Peliti, J. Phys. (Paris) 46 (1985) 1469; Y. Shapir, Y.C. Zhang, J. Phys. Lett. (Paris) 46 (1986) L529.
[15] P.G. Saffman, J. Fluid Mech. 173 (1986) 73; D. Bensimon et al., Rev. Mod. Phys. 58 (1986) 977.
[16] B. Shraiman, D. Bensimon, Phys. Rev. A 30 (1984) 2840; R.C. Ball, M. Blunt, Phys. Rev. A 39 (1989) 3591.
[17] P. Tabeling, G. Zocchi, A. Libchaber, J. Fluid Mech. 177 (1987) 67.
[18] T.A. Witten, L.M. Sander, Phys. Rev. Lett. 47 (1981) 1400; P. Meakin, Phys. Rev. A 27 (1983) 1495.